

## Computed Tomographic Biomarkers in Idiopathic Pulmonary Fibrosis

### The Future of Quantitative Analysis

Xiaoping Wu<sup>1</sup>, Grace H. Kim<sup>2</sup>, Margaret L. Salisbury<sup>3</sup>, David Barber<sup>4</sup>, Brian J. Bartholmai<sup>5</sup>, Kevin K. Brown<sup>6</sup>, Craig S. Conoscenti<sup>7</sup>, Jan De Backer<sup>8</sup>, Kevin R. Flaherty<sup>3</sup>, James F. Gruden<sup>9</sup>, Eric A. Hoffman<sup>10</sup>, Stephen M. Humphries<sup>11</sup>, Joseph Jacob<sup>12,13</sup>, Toby M. Maher<sup>14,15\*</sup>, Ganesh Raghu<sup>16</sup>, Luca Richeldi<sup>17</sup>, Brian D. Ross<sup>18</sup>, Rozsa Schlenker-Herceg<sup>7</sup>, Nicola Sverzellati<sup>19</sup>, Athol U. Wells<sup>14</sup>, Fernando J. Martinez<sup>1,20\*</sup>, David A. Lynch<sup>11</sup>, Jonathan Goldin<sup>2</sup>, and Simon L. F. Walsh<sup>21</sup>

<sup>1</sup>Pulmonary and Critical Care Medicine and <sup>9</sup>Radiology, Weill Cornell Medicine, New York, New York; <sup>2</sup>Radiological Science, University of California Los Angeles School of Medicine, Los Angeles, California; <sup>3</sup>Pulmonary and Critical Care Medicine and <sup>18</sup>Radiology, University of Michigan Hospital, Ann Arbor, Michigan; <sup>4</sup>Computer Science, <sup>12</sup>Respiratory Medicine and <sup>13</sup>Centre for Medical Image Computing, University College London, London, United Kingdom; <sup>5</sup>Radiology, Mayo Clinic, Rochester, Minnesota; <sup>6</sup>Pulmonary, Critical Care, and Sleep Medicine, National Jewish Health, Denver, Colorado; <sup>7</sup>Boehringer Ingelheim Pharmaceuticals, Inc., Ridgefield, Connecticut; <sup>8</sup>FluidDA nv Groeningenlei, Kontich, Belgium; <sup>10</sup>Radiology, University of Iowa Carver College of Medicine, Iowa City, Iowa; <sup>11</sup>Radiology, National Jewish Health, Denver, Colorado; <sup>14</sup>Interstitial Lung Disease Unit, Royal Brompton Hospital, London, United Kingdom; <sup>15</sup>Associate Editor, *AJRCCM*; <sup>16</sup>Pulmonary and Critical Care Medicine, University of Washington Medical Center, Seattle, Washington; <sup>17</sup>Fondazione Policlinico Universitario A. Gemelli, Università Cattolica del Sacro Cuore, Rome, Italy; <sup>19</sup>Radiology, Department of Medicine and Surgery, University of Parma, Parma, Italy; <sup>20</sup>Deputy Editor, *AJRCCM*; and <sup>21</sup>Radiology, Kings College Hospital National Health Service Foundation Trust, London, United Kingdom

ORCID ID: 0000-0002-6910-0718 (X.W.).

Idiopathic pulmonary fibrosis (IPF) is the classic fibrosing interstitial lung disease (ILD). Although inexorably progressive, its natural history is inconsistent and unpredictable (1, 2). This variability in the rate and severity of disease progression makes prognostication for individual patients challenging and creates significant barriers to efficient drug development. Validation of a sensitive, reproducible, and objective biomarker that accurately tracks disease progression and response to therapy would be of enormous benefit. High-resolution computed tomography (HRCT) of the chest is routinely performed in patients with suspected fibrotic lung disease and is widely available, making it a promising target for biomarker research (3). Although there is ample evidence that HRCT provides prognostic information in IPF, qualitative visual assessment is limited by interobserver variability (4). In

contrast, computer-based methods for quantifying disease on HRCT could provide rapid, objective measurement of disease extent and change over time. We convened a group of chest radiologists and pulmonary clinicians with IPF expertise, scientists with expertise in computational image analysis, and key individuals from the pharmaceutical industry to address the optimal approach to developing image-based biomarkers for diagnosis, prognosis, and monitoring of response to therapy in IPF.

## Background

### Imaging Endpoints and Biomarkers in IPF

The Biomarkers Definitions Working Group defines a clinical endpoint as a

variable that reflects how a patient feels, functions, or survives (5, 6). The past 3 decades of IPF clinical trial design have struggled to find a clinical primary endpoint that can be routinely used. Although all-cause mortality is a well-defined, reliable, and easy-to-measure primary endpoint, its use in IPF is limited because of low event rates (7). Therefore, in the absence of an ideal endpoint such as mortality, the substitution of a validated biomarker for a clinical endpoint (i.e., a surrogate endpoint) that can reliably predict the effect of the therapy can significantly improve the efficiency of IPF clinical trials (8–10).

Although quality-of-life and functional status instruments are predictive of mortality and show promise as potential

(Received in original form March 8, 2018; accepted in final form July 6, 2018)

\*Participation complies with American Thoracic Society requirements for recusal from review and decisions for authored content.

Any views expressed in this manuscript represent the personal opinions of the author and not those of Boehringer Ingelheim Pharmaceuticals.

Author Contributions: Conception and design: X.W., G.H.K., F.J.M., J.G., and S.L.F.W. Drafting the manuscript for important intellectual content: X.W., G.H.K., M.L.S., B.J.B., K.K.B., C.S.C., J.D.B., E.A.H., S.M.H., J.J., T.M.M., N.S., A.U.W., D.A.L., J.G., and S.L.F.W. Critical review and editing: X.W., G.H.K., M.L.S., D.B., B.J.B., K.K.B., C.S.C., J.D.B., K.R.F., J.F.G., E.A.H., S.M.H., J.J., T.M.M., G.R., L.R., B.D.R., R.S.-H., N.S., A.U.W., F.J.M., D.A.L., J.G., and S.L.F.W. All authors approved the manuscript.

Correspondence and requests for reprints should be addressed to Simon L. F. Walsh, M.D., National Heart and Lung Institute, Imperial College, Guy Scadding Building, Cale Street, London SW3 6LY, UK. E-mail: slfwalsh@gmail.com.

Am J Respir Crit Care Med Vol 199, Iss 1, pp 12–21, Jan 1, 2019

Copyright © 2019 by the American Thoracic Society

Originally Published in Press as DOI: 10.1164/rccm.201803-0444PP on July 9, 2018

Internet address: www.atsjournals.org

biomarkers, these measures may not reflect therapeutic impact commensurate with survival (6). FVC is widely considered an accepted surrogate endpoint in IPF clinical trials and is routinely used as a primary endpoint. However, it is prone to missing data, it may miss important treatment effects, and, because currently approved therapies affect its rate of decline, its use in future trials may be less compelling (11–13). Quantitative computed tomography (QCT) can be reproducibly performed across the spectrum of disease severity. Currently available data support the ability of QCT to measure baseline disease severity and progression, making it potentially an attractive surrogate endpoint (14, 15).

### Challenges in Qualifying a Biomarker

We seek to establish the clinical value of existing imaging-based biomarkers as prognostic factors (the effects of patient-specific or IPF characteristics on patient outcome), predictive factors (the effects of treatment on IPF), and surrogate endpoints in the setting of IPF (16). As a prognostic factor, it is objectively measurable and might provide information on the likely outcome of IPF in an untreated individual. As a predictive factor, it might provide information on the likely benefit from treatment (either in terms of physiologic outcome or survival). Such predictive factors can be used to identify subpopulations of patients or specific phenotypes that are most likely to benefit from a given therapy.

**Imaging biomarker development and validation.** In the development and qualification of an imaging biomarker, there are three important phases: 1) development (including training of classifiers), 2) analytic validation (determination of cut points, assessment of reproducibility, and evaluation against radiologist measurements), and 3) clinical validation in which the system and its cut points are fixed and it is evaluated against outcomes in new clinical trial data. In the development phase, a supervised classification model is usually constructed using regions of interest with parenchymal abnormalities identified and classified visually by an expert thoracic radiologist. Test validation studies are then performed to estimate the variation of measurement and clarify the cut points for the

intended use of the proposed biomarker. Clinical utility is tested in retrospective then prospective studies to show evidence that the effect of a therapeutic intervention on a clinical endpoint (e.g., mortality) can reliably be predicted by QCT. The final step in this process is qualification of the biomarker by regulatory bodies, such as the U.S. Food and Drug Administration, for use in therapeutic trials and routine clinical practice (17). To date, none of the available QCT methods have completed this process.

## Current Imaging Analysis Methods for IPF Evaluation

### Imaging Protocols

Standardized imaging acquisition is crucial for QCT (18). Volumetric acquisition with contiguous thin section reconstruction is important, with slice thickness usually around 1 mm. Because the depth of inspiration can be a major source of variation, coaching the patient to comply with standardized breathing instructions is critical. Computed tomography (CT) radiation dose used for the acquisition is variable, but can be relatively low, and further reduced by dose modulation. For image reconstruction, a relatively “soft” kernel is used to avoid excessive noise; sharper acquisitions can also be acceptable if a denoising or kernel normalization technique is used (19). Iterative reconstruction techniques are not recommended until the effects of this reconstruction on textural analysis can be clearly understood. To ensure that QCT measurements are comparable, patients should be imaged using the same technique, ideally on the same CT scanner, at all time points. The utility of CT phantom acquisition (20) in clinical trials has not been established but may assist with machine calibration and correct implementation of an acquisition protocol before data collection begins.

### Visual Semiquantitative Scoring

A CT pattern of usual interstitial pneumonia (UIP) is associated with higher mortality in fibrotic lung disease (21–23). In addition, the extent of fibrosis on HRCT has been consistently linked to mortality in IPF in numerous studies

(4, 24–27). Most outcome studies involving HRCT in IPF have focused on the ability of baseline HRCT patterns to predict outcome, but few have evaluated the ability of serial HRCT changes over a specific follow-up period to predict outcome. Semiquantitative HRCT evaluation is prone to inter- and intraobserver variability and may be too insensitive to capture clinically important short-term changes (28).

Despite the large and consistent body of literature indicating a prognostic role for HRCT in IPF, HRCT-based biomarkers are neither routinely used in clinical practice nor incorporated as clinical endpoints in therapeutic trials for several reasons. First, visual assessment of HRCT patterns is subjective, with significant interobserver variation, even among expert radiologists. For example, honeycombing has consistently demonstrated prognostic significance in many studies over the past 15 years (29–33), yet the interobserver agreement for the presence of this pattern is moderate at best (4, 31, 34). Second, it is not yet clear how HRCT pattern and extent can help inform management decisions in an individual patient. Unlike in oncology, where an image-based disease stage maps directly to a management strategy, CT-based staging is not yet routinely used in IPF, although attempts have been made to do so (35–37).

### Computer-based Quantitative Scoring Systems

Although computer-assisted diagnosis algorithms for classifying HRCT patterns have existed for decades (38), recent advances in computer processing power have enabled a groundswell of renewed interest in computer-assisted HRCT image analysis. In recent years, some of these tools have been used to analyze CT imaging data in clinical trials both retrospectively and prospectively. Below is a summary of some of the available computer-based methods for quantifying disease on HRCT that have been used to evaluate clinical trial populations in IPF (Table 1). There is currently no consensus regarding the optimal method for QCT analysis, and this review should not be interpreted as a comparison of their strengths and limitations.

#### **Histogram kurtosis/density measures.**

The Hounsfield unit (HU) scale is a measurement of relative densities

**Table 1.** Summary of Quantitative CT Methods Used in IPF Clinical Trials

QCT Method	Key Findings in IPF
Histogram/kurtosis analysis	1. Kurtosis and skewness on histogram analysis are associated with the changes in physiology and overall survival in patients with IPF (15, 40)
AMFM	<ol style="list-style-type: none"> <li>1. AMFM was shown to be superior to earlier quantitative CT-based metrics, including mean lung density and histogram-based metrics, in distinguishing between normal parenchyma and parenchyma from patients with IPF or sarcoidosis (42)</li> <li>2. AMFM enhanced with 3D texture and a support vector machine classifier was shown to have a better than 90% sensitivity and specificity in classifying five simultaneous regional textures, including emphysema, ground glass, and honeycombing (44, 45)</li> <li>3. AMFM measurement of baseline extent of GGR predicts subsequent disease progression (death, hospitalization, or &gt;10% FVC decline), and postbaseline GGR change correlates with postbaseline FVC change (46)</li> </ol>
CALIPER	<ol style="list-style-type: none"> <li>1. CALIPER ILD variables and vessel-related structures can predict lung function tests and improve on visual CT scores (51, 85)</li> <li>2. Vessel-related structure scores better predict mortality than baseline visual CT scores in IPF (78)</li> <li>3. Compared to IPF alone, patients with combined fibrosis and emphysema do not have worsened outcomes (52) or increased likelihoods of pulmonary hypertension (86) beyond that explained by extents of ILD and emphysema</li> <li>4. CALIPER ILD variables and vessel-related structures better predict lung function decline than longitudinal visual CT scores (55)</li> <li>5. Change in CALIPER features predict survival (87)</li> <li>6. Change in CALIPER features can help distinguish between IPF and NSIP in difficult-to-diagnose cases (88)</li> <li>7. Stability of CALIPER normal lung parenchymal volumes in a phase I therapeutic study (89)</li> </ol>
QLF/QILD	<ol style="list-style-type: none"> <li>1. QLF/QILD measurements have been developed to overcome the variations due to CT technical parameters from the multicenter trials (59)</li> <li>2. QLF scores have been evaluated as the part of the analytic validation with visual scores (59)</li> <li>3. QLF scores have been clinically validated after locking the algorithm (60, 61)</li> <li>4. An automated QLF/QILD system has been implemented and validated to be ready for clinical trials, which is an important part before the clinical utilities (60)</li> <li>5. Changes in QLF and QILD scores were associated with the changes in FVC, FEV<sub>1</sub>, and DL<sub>CO</sub> (surrogate outcomes) (39, 90)</li> <li>6. Week 24 changes in QLF predict FVC changes in Weeks 36 and 48 (61)</li> <li>7. Used in six phase II trials as secondary or exploratory outcomes and one phase IIIb trial as a primary endpoint (72)</li> </ol>
DTA	<ol style="list-style-type: none"> <li>1. DTA fibrosis is associated with visual assessment and baseline lung function, and change in DTA fibrosis extent on sequential scans is associated with change in function (91)</li> <li>2. Greater baseline DTA score is associated with increased risk of disease progression and all-cause hospitalization (63)</li> <li>3. Subjects with disease progression at visual assessment had greater DTA fibrosis extent and poorer lung function at baseline and had greater rates of change in these indexes over the follow-up period (91)</li> <li>4. In two IPF clinical trial populations with sequential scans, an increase of 5.5% in DTA fibrosis extent was associated with progression determined as 5% decline in FVC (unpublished data)</li> </ol>
FRI	<ol style="list-style-type: none"> <li>1. Lobe volumes decrease with progressing disease with lower lobes more affected than upper lobes for all FVC values (71)</li> <li>2. Airway volumes, corrected for lung volumes, increase with progressing disease, with the increase driven by pressure redistribution and traction bronchiectasis (71)</li> <li>3. Lobe volumes and airway volumes could already be severely affected by IPF even when FVC is normal (71)</li> <li>4. Baseline FRI parameters have the potential to predict treatment success (70)</li> <li>5. Endpoints describing changes in regional anatomical structure and function have the potential to be more sensitive than FVC, resulting in smaller and shorter clinical trials (71)</li> </ol>

*Definition of abbreviations:* 3D = three-dimensional; AMFM = Adaptive Multiple Feature Method; CALIPER = Computer-Aided Lung Informatics for Pathology Evaluation and Rating; CT = computed tomography; DTA = Data-Driven Textural Analysis; FRI = Functional Respiratory Imaging; GGR = mixed ground glass plus reticular densities; ILD = interstitial lung disease; IPF = idiopathic pulmonary fibrosis; NSIP = nonspecific interstitial pneumonia; QCT = quantitative CT; QILD = Quantitative Interstitial Lung Disease; QLF = Quantitative Lung Fibrosis.

(attenuation) determined by CT. In the lung parenchyma, CT attenuation, measured in HU, is determined by the relative amounts of air, soft tissue, and blood in each volume element (voxel). The CT histogram provides a distribution of HU for an individual CT image or for the entire lung, permitting calculation of mean lung attenuation, variance, skewness, entropy, and kurtosis. Kurtosis describes the sharpness of the histogram peak and is inversely proportional to the thickness of the two tails

of the histogram. Because lung fibrosis or inflammation causes an increase in the amount of soft tissue in the lung, it will increase mean lung attenuation and thereby decrease the sharpness of the histogram peak (kurtosis) and the degree of leftward skewness of the curve (Figure 1). Mean lung attenuation, skewness, and kurtosis can therefore be used as measures of the extent of lung fibrosis. Generally, a large value of kurtosis indicates mild fibrosis, whereas low kurtosis (i.e., close to 0 or negative) indicates moderate to severe fibrosis (39). Kurtosis and skewness of a histogram are known to be correlated with changes in FVC and overall survival in patients with IPF (15, 40).

#### Adaptive Multiple Feature Method.

The Adaptive Multiple Feature Method (AMFM) is a computer-based texture analysis tool that quantifies lung parenchymal patterns on CT. During development, the AMFM tool was trained on various parenchymal patterns using  $31 \times 31$ -pixel regions of interest (image patches) extracted from CT images (41–43). Ground truth labeling of image patches was provided by the consensus vote of a group of experienced observers (43). During training, the AMFM narrows the texture in a training set image patch to a small number of optimal features for classification, which are then applied to a test set via a Bayesian classifier. The

kappa statistic of agreement between the regions, for which most observers agreed on the pattern type, versus the AMFM tool was 0.62 (43). This technique has been extended to three-dimensional (3D) texture analysis (44, 45) and used to explore the association between the AMFM regional characterization of the lung and outcomes in patients with IPF (46) (Figure 2). Among patients with IPF enrolled in clinical therapeutic trials, both visual and AMFM measurement of baseline extent of mixed ground-glass and reticular (GGR) densities predicted subsequent disease progression (defined as composite death, hospitalization, or  $>10\%$  FVC decline), independent of baseline age, sex, and FVC. In addition, postbaseline change in GGR correlated with postbaseline change in FVC. The authors concluded that the AMFM provides an automated method of supporting existing prognostic markers and can enrich a study population with subjects at greatest risk of disease progression. A challenge, to date, with the application of the AMFM is the alteration of texture by scanning protocols. Legacy data used in the testing of the AMFM to date has required the use of a mixture of scan protocols and poor control of lung volume. More recent multicenter studies have established cross-manufacturer protocols

that serve to more closely align image characteristics (47).

#### Computer-Aided Lung Informatics for Pathology Evaluation and Rating.

The automated lung parenchymal characterization by Computer-Aided Lung Informatics for Pathology Evaluation and Rating (CALIPER) uses a computer vision-based technique that includes volumetric local histogram and morphologic analysis to provide quantitative assessment of pulmonary parenchymal disease on HRCT data. This process automatically labels each pixel of a volumetric HRCT as belonging to one of seven specific parenchymal features: normal, ground-glass opacity, reticular density, honeycombing, and mild, moderate, or severe low-attenuation areas. The CALIPER classifier of lung parenchyma was developed from training sets of pathologically proven ILD and control subjects' HRCT data obtained for the Lung Tissue Research Consortium (LTRC) (48) (Figure 3). Although technical features of acquisition and reconstruction are important to reproducibility of quantitative measures, the CALIPER measures have been shown to be reproducible and robust across a wide variety of acquisition and reconstruction techniques, including low (about 1–2 mSv)- and ultra-low (0.1–0.3 mSv)-dose CT techniques with both filtered back-projection and iterative reconstruction techniques (49).

The CALIPER tool has been used retrospectively on thousands of datasets from multiple institutions and for prospective analysis of approximately 3,000 HRCT scans acquired for the LTRC. It has been successfully used to predict survival and future physiologic change (such as FVC decline) in a variety of fibrotic lung diseases, such as IPF, fibrotic nonspecific interstitial pneumonia, hypersensitivity pneumonitis, unclassifiable ILD, and mixed processes, such as combined pulmonary fibrosis and emphysema (50–55). Furthermore, a CALIPER-derived HRCT measure of “pulmonary vascular-related structures” provides highly discriminative prognostic information in IPF, connective tissue disease-related ILD, hypersensitivity pneumonitis, and unclassifiable ILD. Using additional automated clustering, the CALIPER characterization has been used to phenotype disease and automatically

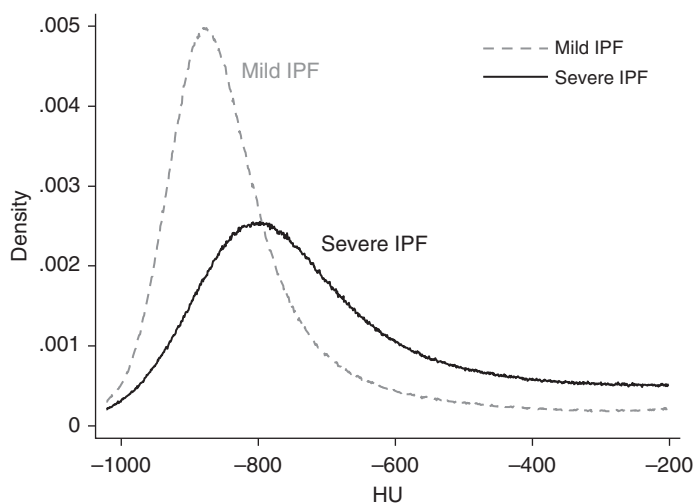


**Figure 1.** Two patients with mild and severe idiopathic pulmonary fibrosis (IPF) (FVC, 65% and 47%, respectively): kurtosis measures are 5.00 and 0.41 in subjects with mild and severe IPF, respectively. Corresponding skewness measures are 1.48 and 0.80. HU = Hounsfield unit. Reprinted by permission from Reference 39.



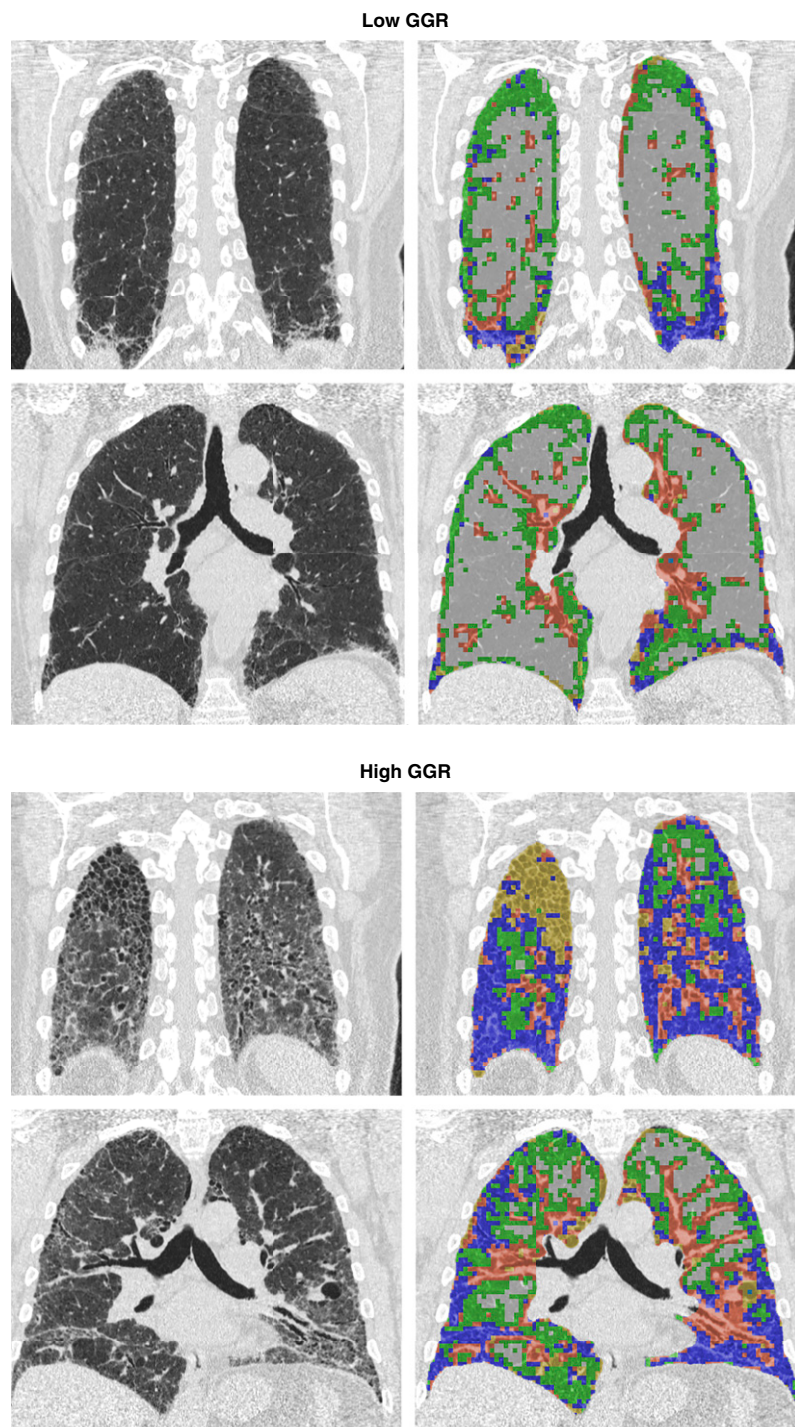


**Figure 2.** Four-panel sets serving as examples of regional Adaptive Multiple Feature Method (AMFM)-derived results for two patients with idiopathic pulmonary fibrosis (IPF). Unlabeled dorsal (top) and midlevel (bottom) coronal sections are shown in the left panels obtained from a subject with lower (top set) and a subject with higher (bottom set) proportion of lung voxels/regions characterized as representing a ground-glass reticular (GGR) texture pattern. The right panels show regional transparent color overlays representing the parenchymal characteristic determined by the AMFM from the regional image texture. A higher proportion of lung characterized as GGR on a baseline high-resolution computed tomography was associated with increased risk of disease progression among subjects with IPF enrolled in a clinical therapeutic trial. Colors represent: ground glass (green), normal (white), ground glass reticular (blue), bronchovascular (brown), and honeycomb (yellow).

stratify subjects into subgroups with prognostic value in 1,322 LTRC scans (56, 57). CALIPER has also been used prospectively in a double-blind, placebo-controlled, phase II clinical trial of a novel antifibrotic drug for IPF, using spirometrically controlled HRCT at baseline and 28 weeks. The mean change in lung volumes and percentage interstitial lung abnormalities (sum of ground-glass, reticular densities, and honeycombing) was evaluated as a secondary endpoint (58).

#### **Quantitative Lung Fibrosis.**

Quantitative Lung Fibrosis (QLF) is part of a panel of measures including quantitative honeycomb, ground-glass, and composite interstitial lung disease (QILD) scores (59). In the discovery phase, the denoised texture features and support vector machine demonstrated robustness in quantitative features across different scanner models and in classifying normal patterns (60). In validation, a five-step process was automated: 1) denoise, 2) voxel sampling, 3) calculate texture features, 4) run support vector machine classifier, and 5) output scores as ratios (percentage) or volumes (milliliters). Analytic validation has been reported: QLF demonstrated a good performance, with visual scoring area under the curve of 0.96 for detection and quantitation of diffuse lung disease and a short-term repeatability coefficient of 0.4% for whole lung and 2% for the most severe lobe within a subject (39, 60, 61). The QLF classifier has used robustness-driven feature selection to improve robustness against slice thickness, reconstruction kernel, and tube current without sacrificing performance. Cut points based on the repeatability measures have been frozen, and QLF and QILD extent at baseline is prognostic of survival and FVC impairment (Figure 4). As surrogate outcomes, QLF and QILD scores have been clinically used in 2,059 HRCT scans from 1,136 subjects in seven IPF clinical trials showing both treatment efficacy and correlation with FVC change.

**Data-Driven Textural Analysis.** Data-Driven Textural Analysis (DTA) is based on unsupervised feature learning and is implemented as a simple convolutional neural network. The convolutional weights are precomputed in an initial

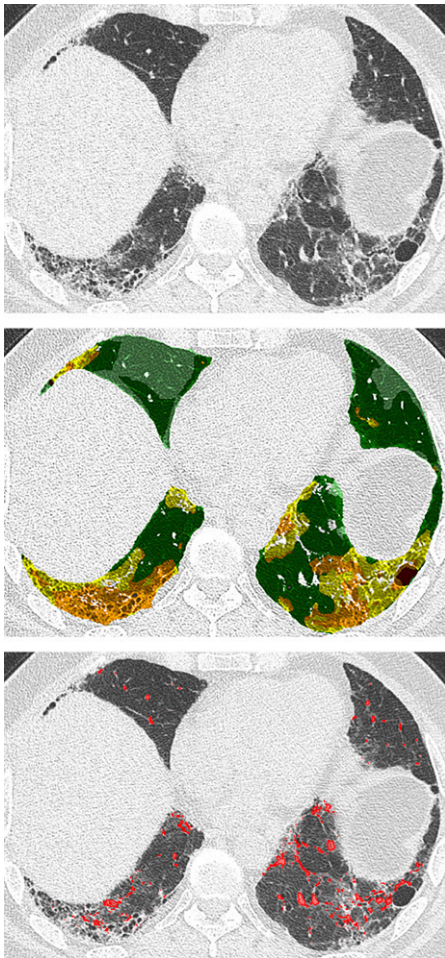


**Figure 3.** Axial computed tomography image of usual interstitial pneumonia with Computer-Aided Lung Informatics for Pathology Evaluation and Rating (CALIPER) characterization. Top: Reticulation, ground-glass opacity, and traction bronchiectasis are visible in both lower lobes and the anterior right middle lobe, with a honeycomb cyst visible in the left lower lobe. Middle: Color overlay image highlighting parenchymal features characterized by CALIPER: normal lung (light and dark green) surrounds areas of ground-glass opacity (yellow), reticulation (orange), and the left lower lobe honeycomb cyst (red). Bottom: Pulmonary vessel volume quantified by CALIPER is an analytic feature that includes pulmonary arteries, veins, and other small branching/linear structures in areas that contain more severe fibrosis.

clustering process on a large collection of unlabeled images (62). The network is trained as a binary classifier using radiologist-labeled regions of interest (ROIs) demonstrating normal

parenchyma and UIP patterns. DTA fibrosis score is calculated as the number of ROIs classified as fibrotic divided by the total number of ROIs sampled from a lung segmentation volume (Figure 5).

Analytic validation in 280 subjects enrolled in IPF Network trials showed that extent of fibrosis measured by DTA correlates with physiologic impairment at baseline (FVC % predicted  $\rho = -0.60$ ,  $P < 0.001$ ; DLCO % predicted  $\rho = -0.68$ ,  $P < 0.001$ ). Responsiveness was tested in a subset of 72 subjects with 15-month follow-up HRCT. Change in DTA score was correlated with change in FVC % predicted ( $\rho = -0.41$ ,  $P < 0.001$ ) and DLCO % predicted ( $\rho = -0.40$ ,  $P < 0.001$ ). Receiver operating characteristic analysis indicated that an increase in DTA score of 5.5% at follow-up identified subjects who experienced a 5% absolute decline in FVC % predicted (63). In a separate retrospective cohort study of 501 subjects with IPF enrolled in an interventional clinical trial, increase in baseline DTA score was associated with increased risk of disease progression and all-cause hospitalization (unpublished data).

#### **Functional Respiratory Imaging.**

Functional Respiratory Imaging (FRI) is a combination of low-dose HRCT scans taken at inspiration and expiration and computer-based flow simulations. The data acquisition procedure includes respiratory gating using a handheld spirometer to ensure correct and repeatable lung volumes (64).

FRI enables regional quantification of lung structure and function and is validated in obstructive lung diseases through comparisons with conventional lung function measures, isotope-based techniques, hyperpolarized helium, exercise tolerance, and patient-reported outcomes (65–67). Test/retest data and repeated baseline scans show very low variability (1–3%) for airway volumes, blood vessel volumes, and airway resistances (68, 69). This low variability is due to the rigorously controlled and respiratory-gated way HRCT scans are obtained, in combination with a standardized 3D reconstruction of the anatomical structures (65) (Figure 6). By focusing on the anatomy (e.g., airway and blood volumes) rather than individual voxels, the variability induced by noise

or reconstruction algorithms associated with low-dose HRCT scans can be reduced.

Recent studies in IPF showed that disease progression, as determined by FVC decline, is associated with a reduction in CT-measured lung volumes ( $R^2 = 0.80$ ,  $P < 0.001$ ) and an increase in relative airway volumes ( $R^2 = 0.29$ ,  $P < 0.001$ ). Changes in FVC are correlated with changes in lung volumes ( $R^2 = 0.18$ ,  $P < 0.001$ ) and changes in relative airway caliber ( $R^2 = 0.15$ ,  $P < 0.001$ ) (70). Lobe and airway volumes can already be significantly affected by IPF, whereas conventional measures such as FVC remain within the normal (healthy) range (71). IPF disease progression manifests itself heterogeneously in terms of FRI parameters, with the lower lobes consistently more affected than the upper lobes. In a recent small drug trial (72) using a novel autotaxin inhibitor, FVC showed a positive but nonsignificant signal of 95 ml between a treatment and placebo arm after 12 weeks of treatment. FRI parameters confirmed the treatment signal with statistical significance. Although FRI is a promising technique, additional studies need to be done to further use FRI as a standard drug development tool and to determine minimal clinically important difference.

#### **Advantages of QCT**

Visual CT features (73), derived from two-dimensional interspaced HRCT imaging in the 1980s (74–77), were primarily designed to provide qualitative information that aided diagnosis. As the focus of CT analysis in ILD moves to prognostication on volumetric baseline and longitudinal CTs, the precision, sensitivity and absence of interobserver variability associated with QCT have made it an increasingly attractive substitute for visual CT analysis. Quantifying subtle changes in CT features using computer analysis is likely to play an important role in the identification of treatment efficacy in an era of newly emerging drug therapies in fibrosing lung disease.

QCT-derived features have outperformed visual CT variables in predicting outcome across several fibrosing lung diseases with diverse radiographic patterns, demonstrating its utility is not limited to the UIP pattern (57, 78, 79). In



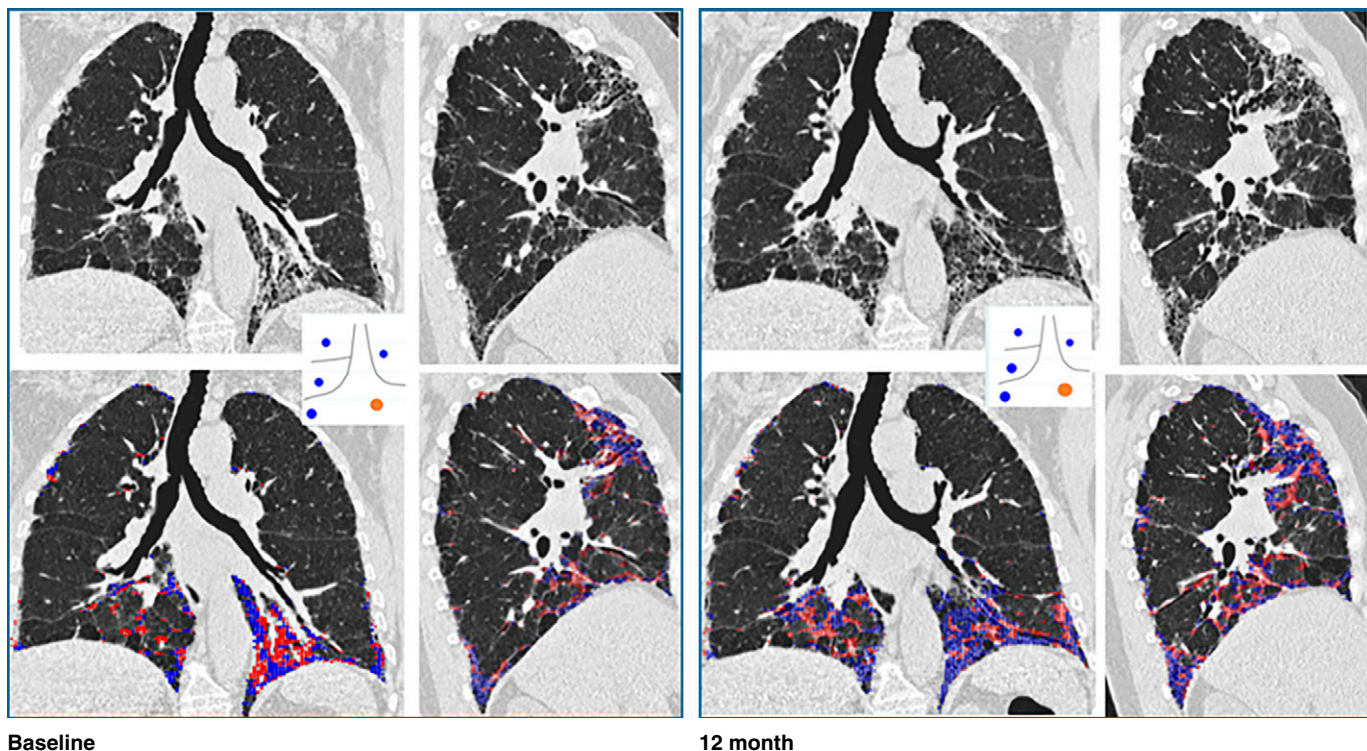


**Figure 4.** Coronal and sagittal computed tomography (CT) images at baseline and 12 months with Quantitative Lung Fibrosis (QLF) characterization. Top: Original images of coronal (left) and sagittal (right) images. Bottom: Annotated coronal and sagittal high-resolution CT images with the classification of QLF (blue and red). Center: A paired set of five-dimensional plots with three-dimensional locations, QLF scores, and temporal information at baseline and 12 months, where the circle size indicates QLF score and an orange circle indicates the most severe lobe (left lower lobe). QLF increased from 12% to 17% in the left lower lobe. In whole lung, QLF increased from 9% to 14% over 12 months.

addition, interrogation of 3D datasets by advanced computer vision and deep learning algorithm techniques may also permit identification of novel biomarkers of disease and prognostic CT features. Rapid and reproducible QCT analysis will likely become increasingly important in

following subjects with interstitial lung abnormalities identified incidentally on CT or during lung cancer screening (80–82).

**Disadvantages of QCT**

QCT has several limitations. First, most published approaches involve

segmentation and feature extraction on the basis of lung density (measured in HU), which is heavily influenced by CT dose, slice thickness, and reconstruction kernel, including new iterative reconstructions (59). Second, patient-related factors, such as inspiratory volume/effort, can significantly impact QCT feature characterization. Thorough coaching of patients regarding inspiratory effort and timing or spirometric control of studies would greatly facilitate reproducibility of results (83) but would significantly increase the complexity of performance in routine clinical practice. Establishing limits of variation, and possibly adjustment for lung volume, may help to resolve this limitation (84). Third, the availability of a noncontrast, volumetric thin high-resolution CT dataset with a CT kernel that does not alter local HU accuracy is essential to accurate feature extraction. This may limit the utility of QCT in retrospective CT datasets, as clinical scans commonly

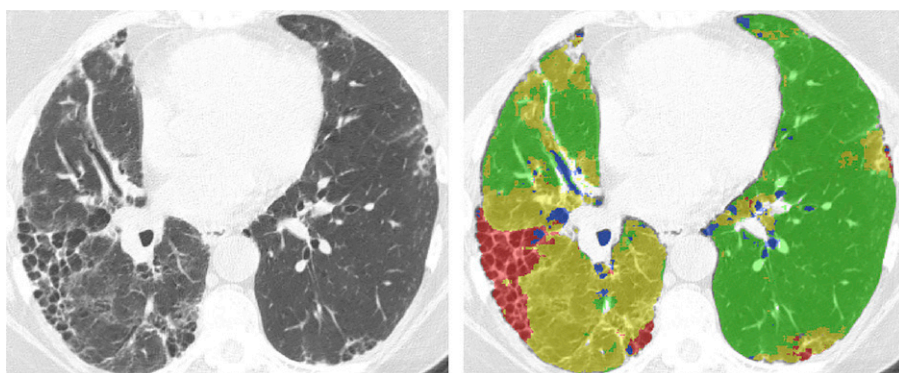


**Figure 5.** Axial chest computed tomography section of a subject with usual interstitial pneumonia (left). Classification results (right) show regions classified as normal (green), airway (blue), reticular abnormality (yellow), and honeycombing (red). Data-Driven Textural Analysis score is the percentage of lung volume occupied by reticular abnormality or honeycombing.

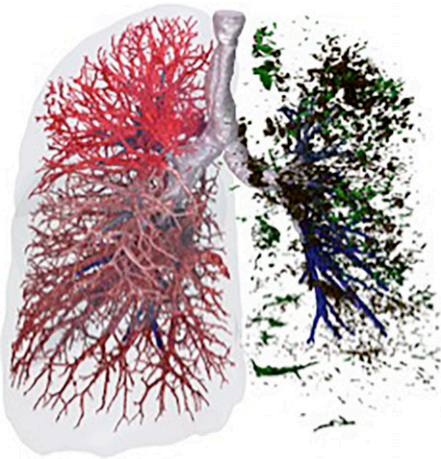


**Figure 6.** Patient-specific reconstruction of fibrosis (green), distal airways (blue), central airways (gray), emphysema (black), and blood vessels (red) using Functional Respiratory Imaging.

are reconstructed with parameters that use edge-enhancing algorithms to increase the visual conspicuity of some pulmonary features.

## Clinical Application of an Image-based Biomarker

The immediate applicability of QCT relates to its potential role in clinical trials. Its use may be considered in the following clinical settings: to stratify patients by disease severity, with theoretical advantages over pulmonary function tests (avoiding the confounding effect of the normal range) and visual HRCT scoring (avoiding interobserver variation), and as a longitudinal predictor of early mortality. Validation would require that serial QCT predict mortality more accurately than serial FVC.

## Conclusions

There is an urgent need to develop sensitive, reproducible, and objective biomarkers in IPF that can be used to monitor disease progression and therapeutic response. QCT provides an objective measure of disease extent and an opportunity to detect

subtle disease progression. Therefore, understandably, QCT has been the focus of intensive biomarker research over the past decade. However, despite a growing body of literature demonstrating the potential of QCT, several questions remain unanswered. First, it is unclear if QCT can predict response to therapy using baseline data in an individual patient with IPF (i.e., QCT is unproved as a predictive factor). Second, QCT has not been shown to reliably identify treatment failure early in a trial of therapy. Although serial QCT has been applied in clinical trials with interesting results, additional prospective biomarker studies will need to be performed to show that progression of fibrosis by QCT can be used as a surrogate outcome biomarker. ■

**Author disclosures** are available with the text of this article at [www.atsjournals.org](http://www.atsjournals.org).

**Acknowledgment:** The authors thank Three Lakes Partners for their support of this manuscript and the Open Source Imaging Consortium.

## References

- Ley B, Collard HR, King TE Jr. Clinical course and prediction of survival in idiopathic pulmonary fibrosis. *Am J Respir Crit Care Med* 2011;183:431–440.
- Fernández Pérez ER, Daniels CE, Schroeder DR, St Sauver J, Hartman TE, Bartholmai BJ, et al. Incidence, prevalence, and clinical course of idiopathic pulmonary fibrosis: a population-based study. *Chest* 2010;137:129–137.
- Hansell DM, Goldin JG, King TE Jr, Lynch DA, Richeldi L, Wells AU. CT staging and monitoring of fibrotic interstitial lung diseases in clinical practice and treatment trials: a position paper from the Fleischner Society. *Lancet Respir Med* 2015;3:483–496.
- Lynch DA, Godwin JD, Safrin S, Starko KM, Hormel P, Brown KK, et al.; Idiopathic Pulmonary Fibrosis Study Group. High-resolution computed tomography in idiopathic pulmonary fibrosis: diagnosis and prognosis. *Am J Respir Crit Care Med* 2005;172:488–493.
- Biomarkers Definitions Working G; Biomarkers Definitions Working Group. Biomarkers and surrogate endpoints: preferred definitions and conceptual framework. *Clin Pharmacol Ther* 2001;69:89–95.
- Raghu G, Collard HR, Anstrom KJ, Flaherty KR, Fleming TR, King TE Jr, et al. Idiopathic pulmonary fibrosis: clinically meaningful primary endpoints in phase 3 clinical trials. *Am J Respir Crit Care Med* 2012;185:1044–1048.
- King TE Jr, Albera C, Bradford WZ, Costabel U, du Bois RM, Leff JA, et al. All-cause mortality rate in patients with idiopathic pulmonary fibrosis: implications for the design and execution of clinical trials. *Am J Respir Crit Care Med* 2014;189:825–831.
- de Benedictis FM, Guidi R, Carraro S, Baraldi E; TEDDY European Network of Excellence. Endpoints in respiratory diseases. *Eur J Clin Pharmacol* 2011;67:49–59.
- Katz R. Biomarkers and surrogate markers: an FDA perspective. *NeuroRx* 2004;1:189–195.
- Temple R. Are surrogate markers adequate to assess cardiovascular disease drugs? *JAMA* 1999;282:790–795.
- Karimi-Shah BA, Chowdhury BA. Forced vital capacity in idiopathic pulmonary fibrosis—FDA review of pirfenidone and nintedanib. *N Engl J Med* 2015;372:1189–1191.
- Wells AU. Forced vital capacity as a primary end point in idiopathic pulmonary fibrosis treatment trials: making a silk purse from a sow's ear. *Thorax* 2013;68:309–310.
- Ley B. Clarity on endpoints for clinical trials in idiopathic pulmonary fibrosis. *Ann Am Thorac Soc* 2017;14:1383–1384.
- Hartley PG, Galvin JR, Hunninghake GW, Merchant JA, Yagla SJ, Speakman SB, et al. High-resolution CT-derived measures of lung density are valid indexes of interstitial lung disease. *J Appl Physiol* (1985) 1994;76:271–277.
- Best AC, Lynch AM, Bozic CM, Miller D, Grunwald GK, Lynch DA. Quantitative CT indexes in idiopathic pulmonary fibrosis: relationship with physiologic impairment. *Radiology* 2003;228:407–414.
- Italiano A. Prognostic or predictive? It's time to get back to definitions! *J Clin Oncol* 2011;29:4718. [Author reply, pp. 4718–4719.]
- US Department of Health and Human Services. Guidance for industry and FDA staff: qualification process for drug development tools. Silver Spring, MD: Food and Drug Administration, Center for Drug Evaluation and Research; 2014.
- Newell JD Jr, Sieren J, Hoffman EA. Development of quantitative computed tomography lung protocols. *J Thorac Imaging* 2013;28:266–271.
- Gallardo-Estrella L, Lynch DA, Prokop M, Stinson D, Zach J, Judy PF, et al. Normalizing computed tomography data reconstructed with different filter kernels: effect on emphysema quantification. *Eur Radiol* 2016;26:478–486.
- Sieren JP, Newell JD, Judy PF, Lynch DA, Chan KS, Guo J, et al. Reference standard and statistical model for intersite and temporal comparisons of CT attenuation in a multicenter quantitative lung study. *Med Phys* 2012;39:5757–5767.
- Kim EJ, Elicker BM, Maldonado F, Webb WR, Ryu JH, Van Uden JH, et al. Usual interstitial pneumonia in rheumatoid arthritis-associated interstitial lung disease. *Eur Respir J* 2010;35:1322–1328.



22. Flaherty KR, Thwaite EL, Kazerooni EA, Gross BH, Toews GB, Colby TV, *et al.* Radiological versus histological diagnosis in UIP and NSIP: survival implications. *Thorax* 2003;58:143–148.
23. Chiba S, Tsuchiya K, Akashi T, Ishizuka M, Okamoto T, Furusawa H, *et al.* Chronic hypersensitivity pneumonitis with a usual interstitial pneumonia-like pattern: correlation between histopathologic and clinical findings. *Chest* 2016;149:1473–1481.
24. Edey AJ, Devaraj AA, Barker RP, Nicholson AG, Wells AU, Hansell DM. Fibrotic idiopathic interstitial pneumonias: HRCT findings that predict mortality. *Eur Radiol* 2011;21:1586–1593.
25. Mogulkoc N, Brutsche MH, Bishop PW, Greaves SM, Horrocks AW, Egan JJ; Greater Manchester Pulmonary Fibrosis Consortium. Pulmonary function in idiopathic pulmonary fibrosis and referral for lung transplantation. *Am J Respir Crit Care Med* 2001;164:103–108.
26. Gay SE, Kazerooni EA, Toews GB, Lynch JP III, Gross BH, Cascade PN, *et al.* Idiopathic pulmonary fibrosis: predicting response to therapy and survival. *Am J Respir Crit Care Med* 1998;157:1063–1072.
27. Sumikawa H, Johkoh T, Colby TV, Ichikado K, Suga M, Taniguchi H, *et al.* Computed tomography findings in pathological usual interstitial pneumonia: relationship to survival. *Am J Respir Crit Care Med* 2008;177:433–439.
28. Flaherty KR, Mumford JA, Murray S, Kazerooni EA, Gross BH, Colby TV, *et al.* Prognostic implications of physiologic and radiographic changes in idiopathic interstitial pneumonia. *Am J Respir Crit Care Med* 2003;168:543–548.
29. Wells AU, Hansell DM, Rubens MB, Cullinan P, Black CM, du Bois RM. The predictive value of appearances on thin-section computed tomography in fibrosing alveolitis. *Am Rev Respir Dis* 1993;148:1076–1082.
30. Sundaram B, Gross BH, Martinez FJ, Oh E, Müller NL, Schipper M, *et al.* Accuracy of high-resolution CT in the diagnosis of diffuse lung disease: effect of predominance and distribution of findings. *AJR Am J Roentgenol* 2008;191:1032–1039.
31. Goldin J, Elashoff R, Kim HJ, Yan X, Lynch D, Strollo D, *et al.* Treatment of scleroderma-interstitial lung disease with cyclophosphamide is associated with less progressive fibrosis on serial thoracic high-resolution CT scan than placebo: findings from the scleroderma lung study. *Chest* 2009;136:1333–1340.
32. Akira M, Inoue Y, Arai T, Okuma T, Kawata Y. Long-term follow-up high-resolution CT findings in non-specific interstitial pneumonia. *Thorax* 2011;66:61–65.
33. Fujimoto K, Taniguchi H, Johkoh T, Kondoh Y, Ichikado K, Sumikawa H, *et al.* Acute exacerbation of idiopathic pulmonary fibrosis: high-resolution CT scores predict mortality. *Eur Radiol* 2012;22:83–92.
34. Sundaram B, Gross BH, Oh E, Müller N, Myles JD, Kazerooni EA. Reader accuracy and confidence in diagnosing diffuse lung disease on high-resolution computed tomography of the lungs: impact of sampling frequency. *Acta Radiol* 2008;49:870–875.
35. Walsh SL, Wells AU, Sverzellati N, Keir GJ, Calandriello L, Antoniou KM, *et al.* An integrated clinicoradiological staging system for pulmonary sarcoidosis: a case-cohort study. *Lancet Respir Med* 2014;2:123–130.
36. Goh NS, Desai SR, Veeraraghavan S, Hansell DM, Copley SJ, Maher TM, *et al.* Interstitial lung disease in systemic sclerosis: a simple staging system. *Am J Respir Crit Care Med* 2008;177:1248–1254.
37. Ley B, Ryerson CJ, Vittinghoff E, Ryu JH, Tomassetti S, Lee JS, *et al.* A multidimensional index and staging system for idiopathic pulmonary fibrosis. *Ann Intern Med* 2012;156:684–691.
38. Rodriguez LH, Vargas PF, Raff U, Lynch DA, Rojas GM, Moxley DM, *et al.* Automated discrimination and quantification of idiopathic pulmonary fibrosis from normal lung parenchyma using generalized fractal dimensions in high-resolution computed tomography images. *Acad Radiol* 1995;2:10–18.
39. Kim HJ, Brown MS, Chong D, Gjertson DW, Lu P, Kim HJ, *et al.* Comparison of the quantitative CT imaging biomarkers of idiopathic pulmonary fibrosis at baseline and early change with an interval of 7 months. *Acad Radiol* 2015;22:70–80.
40. Best AC, Meng J, Lynch AM, Bozic CM, Miller D, Grunwald GK, *et al.* Idiopathic pulmonary fibrosis: physiologic tests, quantitative CT indexes, and CT visual scores as predictors of mortality. *Radiology* 2008;246:935–940.
41. Uppaluri R, Mitsa T, Sonka M, Hoffman EA, McLennan G. Quantification of pulmonary emphysema from lung computed tomography images. *Am J Respir Crit Care Med* 1997;156:248–254.
42. Uppaluri R, Hoffman EA, Sonka M, Hunninghake GW, McLennan G. Interstitial lung disease: a quantitative study using the adaptive multiple feature method. *Am J Respir Crit Care Med* 1999;159:519–525.
43. Uppaluri R, Hoffman EA, Sonka M, Hartley PG, Hunninghake GW, McLennan G. Computer recognition of regional lung disease patterns. *Am J Respir Crit Care Med* 1999;160:648–654.
44. Xu Y, Sonka M, McLennan G, Guo J, Hoffman EA. MDCT-based 3-D texture classification of emphysema and early smoking related lung pathologies. *IEEE Trans Med Imaging* 2006;25:464–475.
45. Xu Y, van Beek EJ, Hwanjo Y, Guo J, McLennan G, Hoffman EA. Computer-aided classification of interstitial lung diseases via MDCT: 3D adaptive multiple feature method (3D AMFM). *Acad Radiol* 2006;13:969–978.
46. Salisbury ML, Lynch DA, van Beek EJ, Kazerooni EA, Guo J, Xia M, *et al.*; IPFnet Investigators. Idiopathic pulmonary fibrosis: the association between the adaptive multiple features method and fibrosis outcomes. *Am J Respir Crit Care Med* 2017;195:921–929.
47. Sieren JP, Newell JD Jr, Barr RG, Bleecker ER, Burnette N, Carretta EE, *et al.*; SPIROMICS Research Group. SPIROMICS protocol for multicenter quantitative computed tomography to phenotype the lungs. *Am J Respir Crit Care Med* 2016;194:794–806.
48. Zavaletta VA, Bartholmai BJ, Robb RA. High resolution multidetector CT-aided tissue analysis and quantification of lung fibrosis. *Acad Radiol* 2007;14:772–787.
49. Raghunath SRS, Karwoski RA, Bruesewitz MR, McCollough CH, Bartholmai BJ, Robb RA. Landscaping the effect of CT reconstruction parameters: robust interstitial pulmonary fibrosis quantitation. *Proceedings - International Symposium on Biomedical Imaging* 2013:374–377.
50. Foley FRS, Rajagopalan S, Karwoski R, Maldonado F, Bartholmai B, Peikert T. Computer-aided lung informatics for pathology evaluation and rating (CALIPER) analysis of chest CT to detect histologically proven emphysema [abstract]. *Am J Respir Crit Care Med* 2016;193:A6613.
51. Jacob J, Bartholmai BJ, Rajagopalan S, Kokosi M, Nair A, Karwoski R, *et al.* Automated quantitative computed tomography versus visual computed tomography scoring in idiopathic pulmonary fibrosis: validation against pulmonary function. *J Thorac Imaging* 2016;31:304–311.
52. Jacob J, Bartholmai BJ, Rajagopalan S, Kokosi M, Maher TM, Nair A, *et al.* Functional and prognostic effects when emphysema complicates idiopathic pulmonary fibrosis. *Eur Respir J* 2017;50:1700379.
53. Moua TRS, Rajagopalan S, Karwoski R, Bartholmai B, Ryu JH, Robb R, *et al.* Can progression of fibrosis as assessed by computer-aided lung informatics for pathology evaluation and rating (CALIPER) predict outcomes in patients with idiopathic pulmonary fibrosis [abstract]? *Chest* 2011;140:1041A.
54. Bartholmai BJ, Raghunath S, Karwoski RA, Moua T, Rajagopalan S, Maldonado F, *et al.* Quantitative computed tomography imaging of interstitial lung diseases. *J Thorac Imaging* 2013;28:298–307.
55. Jacob J, Bartholmai BJ, Rajagopalan S, Kokosi M, Egashira R, Brun AL, *et al.* Serial automated quantitative CT analysis in idiopathic pulmonary fibrosis: functional correlations and comparison with changes in visual CT scores. *Eur Radiol* 2018;28:1318–1327.
56. Raghunath S, Rajagopalan S, Karwoski RA, Maldonado F, Peikert T, Moua T, *et al.* Quantitative stratification of diffuse parenchymal lung diseases. *PLoS One* 2014;9:e93229.
57. Jacob J, Bartholmai BJ, Rajagopalan S, Brun AL, Egashira R, Karwoski R, *et al.* Evaluation of computer-based computer tomography stratification against outcome models in connective tissue disease-related interstitial lung disease: a patient outcome study. *BMC Med* 2016;14:190.
58. Van Den Blink BBB, Wijsenbeek M, Miedema J, Rajagopalan S, Westmore M, Lammering K, *et al.* Automated quantitative imaging correlates with lung function and exercise tolerance in patients with idiopathic pulmonary fibrosis. *QJM* 2016;109:S57.

59. Chong DY, Kim HJ, Lo P, Young S, McNitt-Gray MF, Abtin F, *et al.* Robustness-driven feature selection in classification of fibrotic interstitial lung disease patterns in computed tomography using 3D texture features. *IEEE Trans Med Imaging* 2016;35:144–157.
60. Brown MS, McNitt-Gray MF, Pais R, Shah SK, Qing P, Da Costa I, *et al.* CAD in clinical trials: current role and architectural requirements. *Comput Med Imaging Graph* 2007;31:332–337.
61. Kim GJBM, Weigt S, Belperio JA, Goldin JG. Prediction of IPF using early changes in quantitative imaging patterns using high resolution computed tomography [abstract]. *Am J Respir Crit Care Med* 2016;193:A2706.
62. Coates A, Ng AY. Learning feature representations with k-means. In: *Neural networks: tricks of the trade*. Berlin: Springer; 2012. pp. 561–580.
63. Humphries S, O’Riordan TG, Sundry JS, Zhang JJ, Gong Q, Bayly S, *et al.* Change in CT-derived fibrosis score correlates with lung function progression in a clinical trial population with idiopathic pulmonary fibrosis [abstract]. *Am J Respir Crit Care Med* 2017;195:A6783.
64. Hajian B, De Backer J, Vos W, Van Holsbeke C, Clukers J, De Backer W. Functional respiratory imaging (FRI) for optimizing therapy development and patient care. *Expert Rev Respir Med* 2016;10:193–206.
65. De Backer LA, Vos W, De Backer J, Van Holsbeke C, Vinchurkar S, De Backer W. The acute effect of budesonide/formoterol in COPD: a multi-slice computed tomography and lung function study. *Eur Respir J* 2012;40:298–305.
66. De Backer JW, Vos WG, Vinchurkar SC, Claes R, Drollmann A, Wulfrank D, *et al.* Validation of computational fluid dynamics in CT-based airway models with SPECT/CT. *Radiology* 2010;257:854–862.
67. Tahir BA, Van Holsbeke C, Ireland RH, Swift AJ, Horn FC, Marshall H, *et al.* Comparison of CT-based lobar ventilation with 3He MR imaging ventilation measurements. *Radiology* 2016;278:585–592.
68. Hajian B, De Backer J, Vos W, Van Holsbeke C, Ferreira F, Quinn DA, *et al.* Pulmonary vascular effects of pulsed inhaled nitric oxide in COPD patients with pulmonary hypertension. *Int J Chron Obstruct Pulmon Dis* 2016;11:1533–1541.
69. De Backer J, Van Holsbeke C, Vos W, Vinchurkar S, Dorinsky P, Rebello J, *et al.* Assessment of lung deposition and analysis of the effect of fluticasone/salmeterol hydrofluoroalkane (HFA) pressurized metered dose inhaler (pMDI) in stable persistent asthma patients using functional respiratory imaging. *Expert Rev Respir Med* 2016;10:927–933.
70. Lanclus M, Porter S, Mignot B, Kouchakji E, Gorina E, Van Holsbeke C, *et al.* Late breaking abstract: assessment of disease progression in IPF patients using functional respiratory imaging (FRI) [abstract]. *Eur Respir J* 2017;50:OA1952.
71. Mussche C, Van Holsbeke C, De Backer J, Vos W, Lanclus M, Mignot B, *et al.* Late breaking abstract: responder phenotyping using functional respiratory imaging (FRI) in IPF patients treated with anti-CGTG monoclonal antibody FG3019 [abstract]. *Eur Respir J* 2017;50:PA2811
72. Maher TM, van der Aar EM, Van de Steen O, Allamassey L, Desrivot J, Dupont S, *et al.* Safety, tolerability, pharmacokinetics, and pharmacodynamics of GLPG1690, a novel autotaxin inhibitor, to treat idiopathic pulmonary fibrosis (FLORA): a phase 2a randomised placebo-controlled trial. *Lancet Resp Med* 2018;6:627–635.
73. Hansell DM, Bankier AA, MacMahon H, McLoud TC, Müller NL, Remy J. Fleischner Society: glossary of terms for thoracic imaging. *Radiology* 2008;246:697–722.
74. Müller NL, Guerry-Force ML, Staples CA, Wright JL, Wiggs B, Coppin C, *et al.* Differential diagnosis of bronchiolitis obliterans with organizing pneumonia and usual interstitial pneumonia: clinical, functional, and radiologic findings. *Radiology* 1987;162:151–156.
75. Müller NL, Miller RR, Webb WR, Evans KG, Ostrow DN. Fibrosing alveolitis: CT-pathologic correlation. *Radiology* 1986;160:585–588.
76. Müller NL, Staples CA, Miller RR, Vedral S, Thurlbeck WM, Ostrow DN. Disease activity in idiopathic pulmonary fibrosis: CT and pathologic correlation. *Radiology* 1987;165:731–734.
77. Silver SF, Müller NL, Miller RR, Lefcoe MS. Hypersensitivity pneumonitis: evaluation with CT. *Radiology* 1989;173:441–445.
78. Jacob J, Bartholmai BJ, Rajagopalan S, Kokosi M, Nair A, Karwoski R, *et al.* Mortality prediction in idiopathic pulmonary fibrosis: evaluation of computer-based CT analysis with conventional severity measures. *Eur Respir J* 2017;49:1601011.
79. Jacob J, Bartholmai BJ, Egashira R, Brun AL, Rajagopalan S, Karwoski R, *et al.* Chronic hypersensitivity pneumonitis: identification of key prognostic determinants using automated CT analysis. *BMC Pulm Med* 2017;17:81.
80. Washko GR, Lynch DA, Matsuoka S, Ross JC, Umeoka S, Diaz A, *et al.* Identification of early interstitial lung disease in smokers from the COPDGene Study. *Acad Radiol* 2010;17:48–53.
81. Putman RK, Hatabu H, Araki T, Gudmundsson G, Gao W, Nishino M, *et al.* Evaluation of COPD Longitudinally to Identify Predictive Surrogate Endpoints (ECLIPSE) Investigators; COPDGene Investigators. Association between interstitial lung abnormalities and all-cause mortality. *JAMA* 2016;315:672–681.
82. Ash SY, Harmouche R, Putman RK, Ross JC, Diaz AA, Hunninghake GM, *et al.* COPDGene Investigators. Clinical and genetic associations of objectively identified interstitial changes in smokers. *Chest* 2017;152:780–791.
83. Fuld MK, Grout RW, Guo J, Morgan JH, Hoffman EA. Systems for lung volume standardization during static and dynamic MDCT-based quantitative assessment of pulmonary structure and function. *Acad Radiol* 2012;19:930–940.
84. Obuchowski NA, Reeves AP, Huang EP, Wang XF, Buckler AJ, Kim HJ, *et al.*; Algorithm Comparison Working Group. Quantitative imaging biomarkers: a review of statistical methods for computer algorithm comparisons. *Stat Methods Med Res* 2015;24:68–106.
85. Matsumoto AJ, Bartholmai BJ, Wylam ME. Comparison of total lung capacity determined by plethysmography with computed tomographic segmentation using CALIPER. *J Thorac Imaging* 2017;32:101–106.
86. Jacob J, Bartholmai BJ, Rajagopalan S, Karwoski R, Nair A, Walsh SLF, *et al.* Likelihood of pulmonary hypertension in patients with idiopathic pulmonary fibrosis and emphysema. *Respirology* 2018;23:593–599.
87. Maldonado F, Moua T, Rajagopalan S, Karwoski RA, Raghunath S, Decker PA, *et al.* Automated quantification of radiological patterns predicts survival in idiopathic pulmonary fibrosis. *Eur Respir J* 2014;43:204–212.
88. De Giacomo F, Raghunath S, Karwoski R, Bartholmai BJ, Moua T. Short-term automated quantification of radiologic changes in the characterization of idiopathic pulmonary fibrosis versus nonspecific interstitial pneumonia and prediction of long-term survival. *J Thorac Imaging* 2018;33:124–131.
89. van den Blink B, Dillingh MR, Ginns LC, Morrison LD, Moerland M, Wijsenbeek M, *et al.* Recombinant human pentraxin-2 therapy in patients with idiopathic pulmonary fibrosis: safety, pharmacokinetics and exploratory efficacy. *Eur Respir J* 2016;47:889–897.
90. Ragu G, Scholand MB, de Andrade J, Lancaster L, Mageto Y, Goldin J, *et al.* FG-3019 anti-connective tissue growth factor monoclonal antibody: results of an open-label clinical trial in idiopathic pulmonary fibrosis. *Eur Respir J* 2016;47:1481–1491.
91. Humphries SM, Yagihashi K, Huckleberry J, Rho BH, Schroeder JD, Strand M, *et al.* Idiopathic pulmonary fibrosis: data-driven textural analysis of extent of fibrosis at baseline and 15-month follow-up. *Radiology* 2017;285:270–278.